Orthorhombic Control Laser Beam Migration

Xiang Xiao, Feng Hao, Bin Wang, Fangxiang Jiao, Wenlong Ni, Alex Yeh, and Xinyi Sun, TGS*

Summary

We developed an orthorhombic (ORT) multiarrival control laser-beam migration flow as a model-building engine, with a goal to attain faster computational speeds over standard Gaussian beam or Kirchhoff migration, without sacrifice of frequency, or accuracy. Common-offset data are decomposed and controlled to sparse tau-*p* domain events. ORT kinematic ray tracing is used to construct controlled-width beams (laser beams). The Gaussian beam multiarrival imaging condition is applied. Though the semblance and wavelet are picked and isolated as a small number of seismic elements, a many-to-many mapping from data domain to image domain is adopted, to allow different arrivals for different data slowness (P_m) contributing to a single imaging point. Cleaner migration images are provided in a reduced computation time cycle, for production tomography, by using the laser-thin beam spread approach and by saving the precomputed sparse tau-*p* elements and "timetables" to disk. Included case studies demonstrate the ORT multiarrival capability of this model-building migration flow using synthetic and real data examples from the Gulf of Mexico.

Introduction

Seismic migration maps the recorded wavefield back to its origin at the reflectivity boundary. For model building purposes, ray-based migration has served as a major workhorse due to its fast turnaround capability, and acceptable results. When imaging reservoirs beneath salt bodies or along steep flanks, conventional single-arrival ray-based technology (e.g. Kirchhoff migration) encounters serious problems as the imaging process is not able to reconstruct the scattered energy of the highly irregular (rugose) top salt, and information from waves that pass through the top of a salt mass is effectively lost (or only partially imaged). Wide-azimuth (WAZ), rich-azimuth (RAZ), and full-azimuth (FAZ) data acquisition in the Gulf of Mexico show significant improvement of subsalt images but also bring significantly larger data volumes and high computation costs for a conventional Kirchhoff migration. Beam migration (Hill, 1990, 2001) images the multiarrivals naturally, but also greatly reduces costs of following migrations for tomography iterations, if the dense data volume is decomposed to seismic elements and saved for future iterations. For example, control-beam (Gray et. al, 2009) and hyper-beam (Sherwood et. al, 2009) are routinely used in production. A laser beam migration approach limits the beam spread to a "laser-thin" region (Xiao et al., 2014), and can accommodate large lateral velocity variations to the accuracy of the central rays, while imposing no dip limitations on images. For tomography purposes, some production-beam migration algorithms pick the semblance and save them as a small number of seismic elements. This migration algorithm is simplified as one-to-one mapping from data-domain elements to image-domain elements, or called fast beam migration (Gao et. al., 2006). This method may violate the multiarrival assumption and migration quality is sacrificed. On the contrary, laser beam migration adopts a many-to-many mapping from data domain to image domain, and is capable of migrating multiarrivals to the correct subsurface locations. Therefore laser beam migration offers a more accurate image.

RAZ or FAZ data provide rich azimuthal information that can better describe the subsurface. Harnessing ORT imaging on this data, with azimuthal anisotropy, leads to improved delineation of desirable hydrocarbon targets. ORT-velocity model building and imaging need to be seriously considered where fractures are present due to significant tectonic stresses and uneven stresses in thin-bed layers (Xie et al., 2011). With a nine-parameter tilted-ORT model (Tsvankin, 2001) and an ORT-kinematic ray tracer (e.g., Han et al., 2012), we can handle tilted ORT features in Kirchhoff and beam migration, and use them for velocity model building and imaging. The steeply dipping traps in the Gulf of Mexico can be extremely prolific, capable of being drained with relatively few high-rate wells. The ORT and multiarrival features in complex geologic settings, if not taken into consideration, can yield misleading information about the location and geometry of prospective formations. Conventional imaging seldom provides sufficient information to properly locate an exploration well. As rich-azimuth, full-azimuth surveys proliferate, the demand for ORT multiarrival velocity model building and imaging also increases.

Theory

Traditional TTI models only have five parameters to account for polar anisotropy. Tilted acoustic ORT medium needs nine parameters. Per Tsvankin (2001) they are as follows: $v_0, \varepsilon_1, \delta_1, \varepsilon_2, \delta_2, \delta_3, \alpha, \theta, \varphi$, where v_0 is the slowest velocity along bedding direction x_3; ε_1, δ_1 are the Thomson parameters in the symmetry plane $x_2 - x_3$, the fast set along the crack orientation, ε_2, δ_2 are defined in the symmetry plane $x_1 - x_3$, the second anisotropy parameter set along the slow direction. δ_3 in the plane $x_1 - x_2$ is the transition parameter from fast to slow axis; α, θ, φ are the dip, azimuth, and fractural directions to rotate the stiffness tensor from the symmetry axis to Cartesian coordinates. We use the kinematic ray-tracing system (Červený, 1972, 2001) in Equation 1 and the ORT parameters listed above to compute the phase velocity and group velocity, and solve the raypath vector x_i and slowness vector $p_i = \partial T/\partial x_i$:

$$\begin{cases} \frac{dx_i}{dT} = \alpha_{ijkl} p_l g_j g_k \\ \frac{dp_i}{dT} = -\frac{1}{2}\frac{\partial \alpha_{jkln}}{\partial x_i} p_k p_n g_j g_l \end{cases} \quad i,j,k,l,n \in \{1,2,3\}. \qquad (1)$$

Here T is the traveltime along the raypath $\vec{x}$, $\alpha_{ijkl} = c_{ijkl}/\rho$ is the density normalized elastic parameter and c_{ijkl} is the stiffness tensor, g_i is the normalized eigenvector, which satisfies the Christoffel equation $(\Gamma_{ik} - \delta_{ik})g_k = 0$ with Chistoffel matrix $\Gamma_{ik} = \alpha_{ijkl} p_j p_l$. This is similar to Cheng et. al (2012) except only acoustic-ORT conditions are assumed to reduce complexity and to improve efficiency. After ORT-kinematic ray tracing on predefined source/receiver grids, "timetables" can be saved to disk and interpolation is used at the migration stage to get the "Green's function" at the actual source and receiver positions.

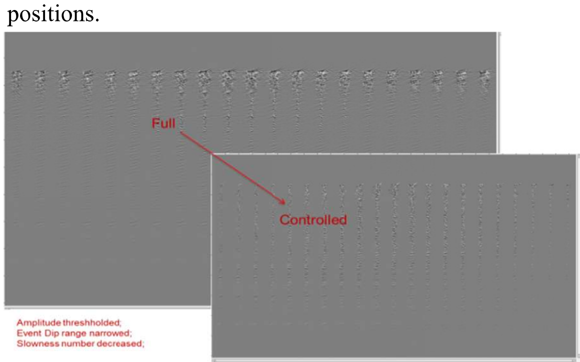

Figure 1: Tau-p domain controls of a 3D NAZ data example.

For a production scale migration, controls are always needed to reduce the artifacts, improve and/or balance the accuracy and efficiency. For a tomography-oriented control laser-beam migration, we not only control the beam width to a laser thin neighborhood to improve the accuracy, but also pick the semblance and wavelet then reduce the seismic data to a small number of seismic elements. A many-to-many mapping from data domain to image domain is adopted, by allowing different arrivals for different data slowness P_m repositioning to the same imaging points. Some further controls are: set threshold of the tau-*p* data, narrow the event dip range, decrease the slowness number, and select by dip steering. A 3D example of tau-*p* domain control (Figure 1) shows that sparse events are preserved.

Demonstrated in Figure 2, the control Laser-beam is implemented as follows:

Step 1: Decompose the tapered common-offset wavefield near a beam center into local plane waves by local slant stacking. After necessary data clipping and preprocess filtering, wavelet shaping is used to get a zero-phase output image from zero-phase input data. If the data is regularized, fast FFT calculation can be used in tau-p transform to speed up the decomposition, instead of a slow version of irregular beam-forming with X-T domain local slant stacking. We then apply data-based controls: pick the semblance and wavelet and isolate the seismic data to a small number of seismic elements.

Step 2: Approximate the propagation of the seismic wavefield using laser beams. On predefined source/receiver grids, we first perform kinematic raytracing for the central rays, and then extrapolate using a Taylor expansion to get the "timetables" T and T* (Traynin et. al, 2008). Finally we save them to disk as "Green function" for future interpolation.

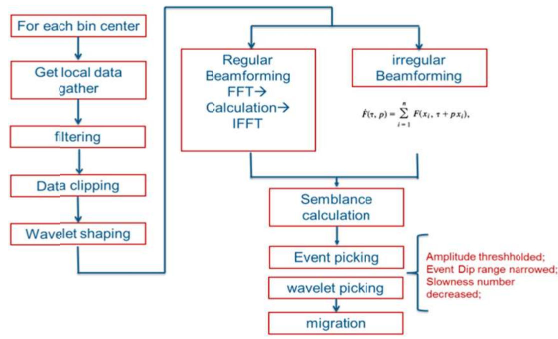

Figure 2: Control beam flow scratch.

Step 3: Migrate the tau-p domain elements using the Gaussian beam multiarrival imaging condition (Hill, 1990, 2001). Model based dip steering is applied to throw away those data elements with conflicting image dips from the known model dips. Only prominent data elements with significant energy are mapped to image domain and cleaner migration images are achieved. Those trivial events, or energy in the seismic data are ignored to achieve a reduced computational cycle time, for production tomographic purposes.

Step 4: Stack the partial images within each offset to form the offset gather and use them in the CIG-based reflection tomography.

Numerical Tests

2D Sigsbee data

We first applied control laser beam migration on decimated 2D Sigsbee dataset (1/20 of total), with production parameters and compared it to our production final laser beam migration with full original dataset (Figure 3). As expected, most prominent events are preserved; thus our control laser beam migration can be used safely in tomography iterations. Since this is a synthetic data set, no noise reduction can be observed in control laser-beam

DOI http://dx.doi.org/10.1190/segam2014-1443.1

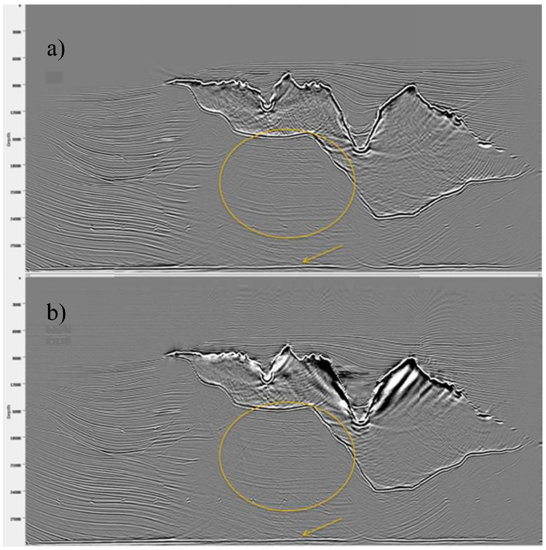

Figure 3. Sigsbee production migration results: (a) final laser-beam migration and (b) control laser-beam migration.

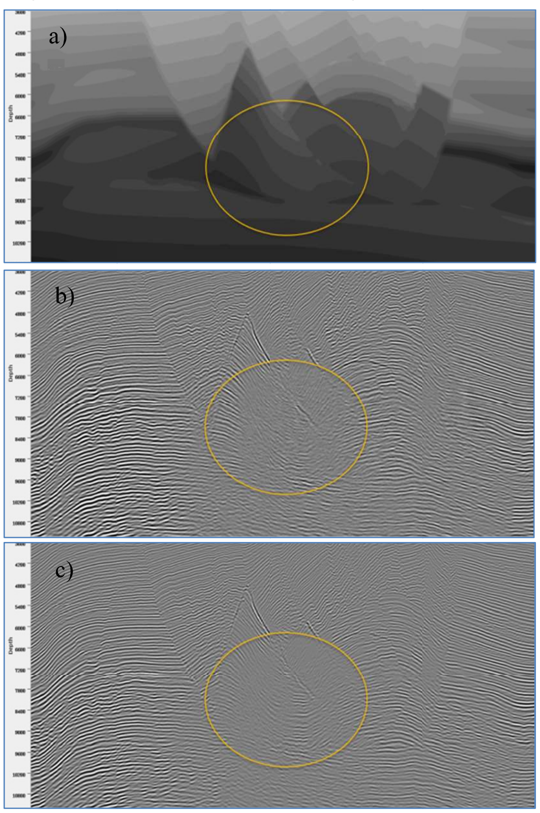

Figure 4: (a) Zoom view of velocity model, (b) TTI Kirchhoff and (c) ORT beam migration results.

migration. Simple offset muting is applied in the control laser-beam migration.

BP 2007 model

We also applied our ORT control laser-beam migration to the BP 2007 synthetic data set and compared it to our final TTI Kirchhoff migration (Figure 4). This comparison demonstrates that by combining multiarrivals and ORT together, control laser-beam can delineate faults clearer and layers more coherent in strong anisotropic areas.

3D Kepler OWAZ data

The Kepler and Justice orthogonal WAZ (OWAZ) surveys were acquired offshore Louisiana in the Mississippi Canyon, Gulf of Mexico. The study area here is dominated by a large overhanging salt body, which created many faults and parallel fractures in surrounding layers. These complex geology settings cause uneven stress and introduce azimuthal anisotropy. With ORT model building and ORT Kirchhoff migration (He et. al, 2013), the conflicting moveouts among gathers from different azimuths with TTI model are flattened using an ORT model with simpler geologic structures. We then applied ORT control laser beam migration to this model and compared with the original ORT Kirchhoff migration (Figure 5). It's obvious that control laser beam migration has better coherency and less migration noise. Faster speed, more coherent migration events in both migration image and offset gather (Figure 6), make the control laser beam

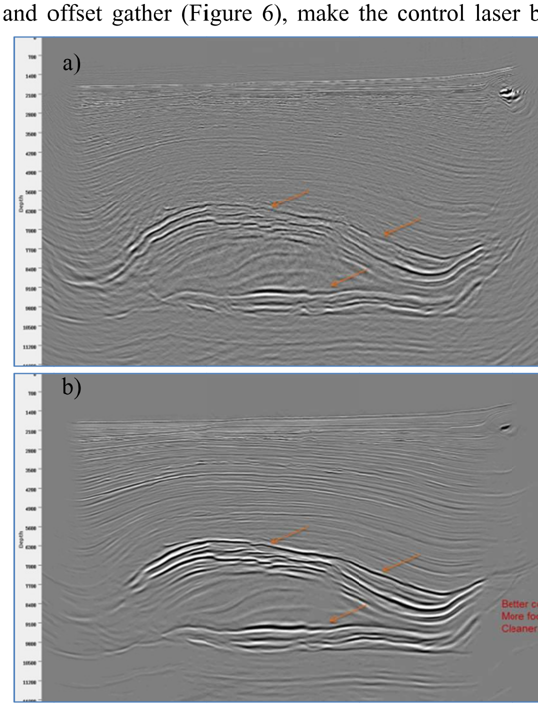

Figure 5: 3D Kepler OWAZ migration results: (a) ORT Kirchhoff migration, and (b) ORT beam migration.

DOI http://dx.doi.org/10.1190/segam2014-1443.1

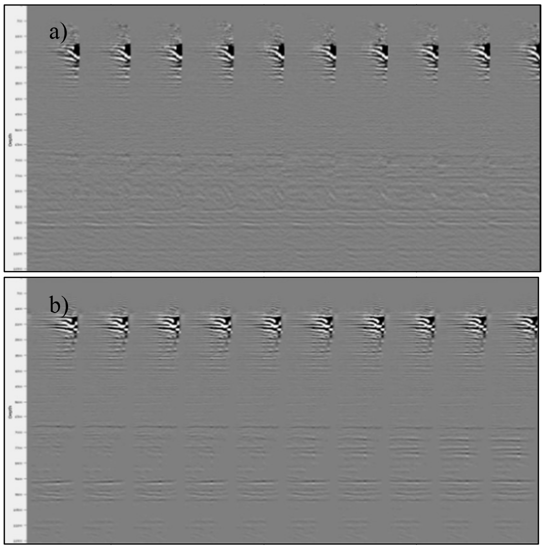

Figure 6: 3D Kepler OWAZ ORT migrations: (a) Kirchhoff gather and (b) beam gather.

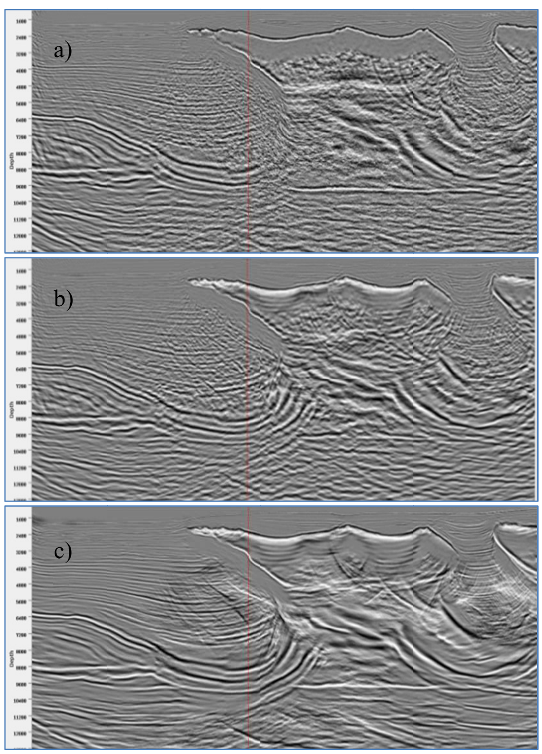

Figure 7: Kepler OWAZ TTI migration results: (a) Final Kirchhoff migratoin, (b) Final laser beam migration and (c) control laser beam migration.

migration the best candidate for the tomography engine. TTI migration comparisons in another study area also demonstrate the same conclusions (Figures 7 and 8).

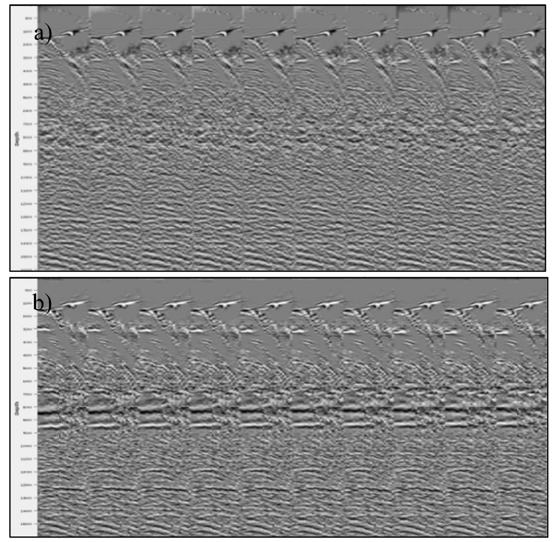

Figure 8: 3D Kepler OWAZ TTI migration gather: (a) Kirchhoff gather and (b) control laser-beam gather.

Without decimation, the control laser beam migration is about 3X faster than the original final laser beam migration. With decimation, more speedup is achieved.

Conclusions

We developed an ORT multiarrival control laser beam flow and demonstrated its model building capability by successfully applying it on both 2D synthetic data sets and Kepler 3D OWAZ data. The ORT control laser beam images are superior to those from a single arrival Kirchhoff migration or standard Gaussian beam migration with production parameters. Over 3X speedup over final laser beam migration while processing 3D WAZ data sets, demonstrates its effectiveness as a model-building engine.

Acknowledgements

We would like to thank Zhiming Li, Simon Baldock, Gary Rodriguez, James Sheng, Jean Ji, Yang He, Manhong Guo and Yongbo Zhai for their valuable suggestions. We thank Terry Hart, Greg Abarr, Cristina Reta-Tang, Taejong Kim, Jianli Song, Jianshun Sheng and Xinling Wang for using control laser-beam migration on NAZ and WAZ velocity model building. We thank Connie VanSchuyver, Chris Egger and Jeff Sposato for proof-reading this paper. We thank TGS management for permission to publish this paper. We also thank Dave Hale and Robert Nowack for the advice and consortium support.

http://dx.doi.org/10.1190/segam2014-1443.1

EDITED REFERENCES

Note: This reference list is a copy-edited version of the reference list submitted by the author. Reference lists for the 2014 SEG Technical Program Expanded Abstracts have been copy edited so that references provided with the online metadata for each paper will achieve a high degree of linking to cited sources that appear on the Web.

REFERENCES

Cervený, V., 1972, Seismic rays and ray intensities in inhomogeneous anisotropic media: Geophysical Journal of the Royal Astronomical Society, **29**, no. 1, 1–13, http://dx.doi.org/10.1111/j.1365-246X.1972.tb06147.x.

Cervený, V., 2001, Seismic ray theory: Cambridge University Press.

Cheng, X., J. Tang, L. Zdraveva, C. E. Yarman, and J. Hobro, 2012, Ray-based prestack depth migration for orthorhombic media: 82nd Annual International Meeting, SEG, Expanded Abstracts, doi: 10.1190/segam2012-0721.1.

Gao, F., P. Zhang, B. Wang, and V. Dirks, 2006, Fast beam migration — A step toward interactive imaging: 76th Annual International Meeting, SEG, Expanded Abstracts, 2470–2474.

Gray, S., Y. Xie, C. Notfors, T. Zhu, D. Wang, and C. Ting, 2009, Taking apart beam migration: The Leading Edge, **28**, 1098–1108, http://dx.doi.org/10.1190/1.3236380.

Han, W., and S. Xu, 2012, Raytracing and traveltime calculations for orthorhombic anisotropic media: 74th Conference & Exhibition, EAGE, Extended Abstracts, A023.

He, Y., A. Gersztenkorn, S. Yang, B. Wang, and X. Xiao, 2013, Orthorhombic imaging for orthogonal wide azimuth surveys in Mississippi Canyon, Gulf of Mexico: 75th Conference & Exhibition, EAGE, Extended Abstracts, doi: 10.3997/2214-4609.20130608.

Hill, N. R., 1990, Gaussian beam migration: Geophysics, **55**, 1416–1428, http://dx.doi.org/10.1190/1.1442788.

Hill, N. R., 2001, Prestack Gaussian-beam depth migration: Geophysics, **66**, 1240–1250, http://dx.doi.org/10.1190/1.1487071.

Sherwood, J., K. Sherwood, H. Tieman, and K. Schleicher, 2008, 3D beam prestack depth migration with examples from around the world: 78th Annual International Meeting, SEG, Expanded Abstracts, 438–442.

Traynin, P., J. Liu, and J. M. Reilly, 2008, Amplitude and bandwidth recovery beneath gas zones using Kirchhoff prestack depth Q-migration: 78th Annual International Meeting, SEG, Expanded Abstracts, 2412–2416.

Tsvankin, I., 2001, Seismic signatures and analysis of reflection data in anisotropic media: Elsevier.

Xiao, X., F. Hao, C. Egger, B. Wang, F. Jiao, and X. Wang, 2014, Final laser-beam Q-migration: 84th Annual International Meeting, SEG, Expanded Abstracts, http://dx.doi.org/10.1190/segam2014-1432.1

Xie, Y., S. Birdus, J. Sun, and C. Notfors, 2011, Multi-azimuth seismic data imaging in the presence of orthorhombic anisotropy: 73rd Conference & Exhibition, EAGE, Extended Abstracts, G022.